agronomy

MDPI

Article

Integrative Transcriptomic and Proteomic Analyses of Quality Differences in Wheat Cultivars Grown in Two Ecological Regions

Anding Zhou [1,2], Yanyan Ren [2], Lianzheng Liu [2], Junmei Cao [2], Na Liu [2], Halidan Yikeremu [2], Na Sun [3], Yanming Shang [4], Qiannan Huang [3], Li Wu [4], Mingshan You [1,*] and Xinzhong Zhang [2,*]

1 Key Laboratory of Crop Heterosis and Utilization (MOE) and Beijing Key Laboratory of Crop Genetic Improvement, China Agricultural University, Beijing 100193, China; zadxyz@163.com
2 Institute of Crop Research, Academy of Agricultural Sciences of Xinjiang Uyghur Autonomous Region, Urumqi 830091, China; renyanyan2025@163.com (Y.R.); lzhliu1985@163.com (L.L.); caojm0508@126.com (J.C.); liunakaixin2009@163.com (N.L.); halida9@163.com (H.Y.)
3 Yili Prefecture Institute of Agricultural Science, Yining 835000, China; sna18509993321@163.com (N.S.); qiannan9325@163.com (Q.H.)
4 Tacheng Prefecture Agricultural Science Research Institute, Tacheng 834700, China; 18099306660@163.com (Y.S.); 13399739009@163.com (L.W.)
* Correspondence: msyou67@cau.edu.cn (M.Y.); zxinzhong1031@163.com (X.Z.)

Abstract

Advancements in the grain industry and evolving dietary patterns have made the processing quality of wheat a key determinant governing the diversification and industrial application of flour products. Characterizing genotype-dependent environmental responses is important for quality-oriented breeding of high-quality bread wheat. In this study, two winter wheat cultivars with distinct gluten properties—the strong-gluten Xindong 23 and the medium-gluten Xindong 53—were grown in two ecological regions of Xinjiang (Yili and Tacheng) during the 2024–2025 season. Integrative transcriptomic and proteomic analyses were performed on developing grains at three nominal grain-filling stages (10, 20, and 30 days after anthesis). Blocked factorial analysis detected genotypic differences, site effects and genotype-by-site interactions for six of eight processing quality traits. Specifically, Xindong 23 exhibited superior processing quality potential but displayed substantial ecological variation between the two experimental sites. In contrast, Xindong 53 showed smaller site-associated differences in several rheological traits within this trial. Multi-omics analysis further showed extensive site-associated transcriptomic and proteomic responses in Xindong 23. In Xindong 23, endoplasmic reticulum protein processing and ribosome-related pathways were enriched at early and middle grain filling, respectively. Direct transcript–protein matching showed positive, stage-dependent agreement, including a concordant omega-gliadin candidate at middle filling. Collectively, this study identifies candidate molecular associations with cultivar-specific quality responses, providing preliminary evidence for further environmental trials and functional investigation of specialized wheat varieties.

Keywords: wheat; processing quality; G × E interaction; multi-omics; ecological adaptability

Check for updates

Academic Editor: Mirosław Tyrka

Received: 24 August 2026
Revised: 8 October 2026
Accepted: 14 October 2026
Published: 9 November 2026

Copyright: © 2026 by the authors. Licensee MDPI, Basel, Switzerland. This article is an open access article distributed under the terms and conditions of the Creative Commons Attribution (CC BY) license.

1. Introduction

As a paramount staple crop worldwide, wheat supplies approximately 20% of human dietary calories and proteins, underpinning global food security and nutritional health [1,2]. Distinct from other cereals, the unique viscoelasticity of wheat dough enables the production of diverse flour-based foods, making it essential for global dietary diversity and the

agricultural economy [3]. The demand for high-quality specialized wheat highlights the importance of developing cultivars with appropriate processing properties [4]. Therefore, elucidating the mechanisms underlying wheat quality formation is of great theoretical and practical significance for developing domestic premium wheat varieties and alleviating this supply shortage.

Wheat quality encompasses both nutritional and processing quality; this study focuses specifically on processing quality [5,6]. Processing quality dictates the rheological and baking properties of wheat during food manufacturing and serves as the core determinant of end-product quality. It is comprehensively evaluated through multiple indices, including grain protein content, dough development time, dough stability time, and extensograph energy [7,8]. According to the Chinese national standard (GB/T 17320–2013), strong-gluten wheat requires a protein content ≥ 14%, dough stability time ≥ 8 min, and extensograph energy ≥ 90 cm^2 [9]. However, most wheat cultivars currently grown in China exhibit intermediate values for these indicators, resulting in a severe scarcity of specialized varieties. Developing a deeper understanding of the mechanisms governing quality formation, coupled with the establishment of robust breeding and cultivation systems, is crucial for resolving this shortage [10,11].

Wheat processing quality is primarily governed by the composition and quantity of grain storage proteins, which dictate wet gluten content and dough rheological properties [7,12]. Gluten proteins consist of glutenins and gliadins: gliadins confer dough viscosity and extensibility, whereas glutenins form large disulfide-crosslinked networks that endow dough with strength and elasticity. Glutenins are classified into high-molecular-weight (HMW-GS) and low-molecular-weight (LMW-GS) subunits, while gliadins are predominantly monomeric proteins comprising ω-, α/β-, and γ-gliadin subgroups [13,14]. In common wheat, HMW-GSs are encoded by loci on chromosomes 1A, 1B, and 1D (*Glu-A1*, *Glu-B1*, and *Glu-D1*), with specific allelic combinations exerting significant effects on dough and bread quality [15]. The LMW-GS gene family, encoded by the *Glu-A3*, *Glu-B3*, and *Glu-D3* loci, is strongly associated with dough extensibility [16,17]. However, the precise contribution of gliadins to dough quality is highly dependent on their specific subunit composition and spatiotemporal expression patterns. While certain gliadins contribute to dough viscosity, excessive accumulation of specific subgroups, such as ω- and α-gliadins, is widely recognized to negatively impact dough strength. Consequently, deficiencies in ω-gliadin genes (*Gli-A1*, *Gli-B1*, *Gli-D1*) [18] or the α-gliadin gene *Gli-D2* [19] can substantially improve dough quality. Additionally, epigenetic modifications, such as the DNA methylation-mediated reduction of *TaGli-γ-2.1* expression, significantly prolong dough stability time [20]. Beyond structural genes, transcription factors like *TaGAMyb* and *TaNAC019* have been identified as key positive regulators of glutenin accumulation and dough stability [21,22]. Nevertheless, how these known quality-related networks are coordinated across growing environments remains incompletely understood. Transcript abundance does not necessarily predict protein abundance because of post-transcriptional regulation and protein turnover; combining transcriptomics and proteomics therefore provides complementary evidence on quality-related responses.

Genotype (G) provides the genetic basis for wheat quality, while the ecological environment (E) acts as a crucial exogenous driver of phenotypic plasticity. Multiple environmental factors, including temperature, sunshine duration, light intensity, soil moisture, and precipitation patterns, profoundly influence quality formation [23,24]. For instance, high temperatures during grain filling reduce starch accumulation but increase grain protein content, whereas cold stress inhibits the accumulation of both [25]. Light intensity alters the abundance and composition of storage proteins, affecting dough rheology [26], while moderate drought can promote the accumulation of specific storage proteins (e.g., HMW-GS

Dy12) to improve processing quality [27]. Overall, wheat quality is a complex quantitative trait synergistically regulated by G, E, and their interaction (G × E), with G × E interactions reflecting non-additive genotype and environment effects, such that genotypes differ in their responses to an environmental contrast [28]. Although the individual effects of ecological factors on wheat quality have been documented, geographical site comparisons capture combined weather, soil and management effects rather than an isolated environmental driver. The coordination of transcript and protein responses with quality traits during grain filling remains incompletely resolved. Dough stability time reflects mixing tolerance and is evaluated here alongside protein, gluten and extensograph traits.

To address these knowledge gaps, two winter wheat cultivars with distinct gluten properties—strong-gluten Xindong 23 and medium-gluten Xindong 53—were cultivated in two ecologically distinct regions of Xinjiang (Yili and Tacheng). Grain samples were collected at three nominal grain-filling stages (10, 20, and 30 days after anthesis, DAA) for integrative transcriptomic and proteomic analyses. By focusing on core biological pathways, including gluten protein synthesis, ribosome biogenesis, and endoplasmic reticulum protein folding, we characterized cultivar-specific site responses and formally tested genotype-by-site interactions. Furthermore, we screened candidate genes associated with the site responses of wheat processing quality. This study aims to provide candidate pathways and genes for subsequent investigation and quality-oriented breeding of wheat.

2. Materials and Methods

2.1. Plant Materials and Experimental Design

The field trial included seven winter wheat cultivars; Xindong 23 and Xindong 53 were selected for this study after examining the seven-cultivar quality results, based on their contrasting processing-quality profiles (Table S1). The strong-gluten cultivar Xindong 23 was bred by the Institute of Nuclear Technology and Biotechnology, Xinjiang Academy of Agricultural Sciences, and developed via anther culture from a cross between an introduced American wheat germplasm and the independently bred wheat line 88-136. The medium-gluten cultivar Xindong 53, a high-quality variety optimized for noodle processing, was bred by the Institute of Crop Research of the same academy through a combined strategy of pedigree selection and marker-assisted selection, with the self-developed line 01-2113 as the female parent and the elite strong-gluten cultivar Xindong 18 as the male parent. Seeds for both cultivars were supplied by the Institute of Crop Research, Xinjiang Academy of Agricultural Sciences.

Field experiments were conducted at two experimental sites in Yili and Tacheng during the 2024–2025 growing season. The Yili site was located at 43°54′ N, 81°16′ E and 639 m above sea level, while the Tacheng site was located at 46°42′46.2″ N, 87°57′11.7″ E and 516 m. Trial-site meteorological records were aligned to the actual flowering and sampling dates (Table S2). Tacheng records supplied daily temperature extrema, rainfall and sunshine, while Yili logger records supplied temperature and relative-humidity summaries with recording coverage. The different measurement definitions are retained separately in Table S2.

A randomized complete block design was applied for field arrangement, with seven cultivars, three blocks at each site and a plot area of 12 m^2. Each plot comprised 10 rows, 6 m long and 20 cm apart. Manual row sowing used 630 seeds per row, corresponding to 350,000 seeds per mu (approximately 525 seeds m^{-2}). Yili was sown on 30 September 2024 and Tacheng on 4 October 2024. All field management practices, including irrigation, fertilization, and pest, disease, and weed control, were implemented in accordance with local standard cultivation protocols and formed part of the overall site conditions. Grains were sampled at nominal 10, 20 and 30 DAA for subsequent transcriptomic and proteomic

analyses. For clarity, grain samples from Xindong 23 and Xindong 53 grown in Tacheng were designated as E and D, respectively, whereas those cultivated in Yili were designated as Ta1 and Ta4. Sample suffixes 1, 2 and 3 correspond one-to-one to field blocks I, II and III. Mature grains from the remaining plants were harvested, threshed, cleaned, and stored at room temperature for the determination of wheat processing quality traits.

2.2. Determination of Flour Quality Traits

The harvested grains were air-dried naturally to a moisture content of 12–14%. A total of 1 kg of purified wheat grains was accurately weighed and milled using a Brabender flour mill (Brabender, Duisburg, Germany). Flour fractions passing through a 100-mesh standard sieve were collected, hermetically sealed, and stored at 4 °C. All quality indices were determined within 24 h after sample preparation.

The dry-based protein content was determined using a DA7250 near-infrared grain quality analyzer (Perten, Hägersten, Sweden) in accordance with the AACC Official Method 39-11 [28]. Wet gluten content and gluten index were measured with a GM2200 gluten analyzer (Perten, Hägersten, Sweden) [29].

Dough farinograph parameters were determined using a Farinograph-E instrument equipped with a 10 g mixing bowl (Brabender, Germany), following the Chinese national standard GB/T 14614-2019 [30]. Dough extensograph properties were tested using an Extensograph-E device (Brabender, Germany) according to GB/T 14615-2019 [31].

For 1000-kernel weight, a cleaned, mixed seed sample was randomly subsampled to 500 kernels, weighed with a 0.01 g balance and doubled. Three repetitions were averaged; if their calculated 1000-kernel weights differed by 0.05 g or more, sampling was repeated. Grain width and length were measured in three repetitions by aligning 10 representative whole kernels in the corresponding dimension, measuring the combined span with a 0.01 mm calliper and dividing by 10. The mean of the three measurement-specific length/width ratios was used. Subsamples were averaged within plots, and dimensions are reported in millimetres (Table S3).

Quality traits were analysed using a blocked factorial model: $y = \mu + \text{genotype} + \text{site} + \text{genotype} \times \text{site} + \text{block(site)} + \text{error}$. The field plot was the biological unit (12 focal plots; residual df = 4). Tables 1–3 report model contrasts, unadjusted 95% confidence intervals and Benjamini–Hochberg (BH) q values, correcting across eight traits within each contrast. Post-screening sensitivity and model diagnostics are provided in Table S1. For each trait, CV (%) was calculated within each site as the sample standard deviation of the three block values divided by their mean × 100, then averaged over the two sites. The final average CV is the arithmetic mean of these eight trait CVs; it describes within-site block dispersion.

Table 1. Quality index differences between Xindong 23 and Xindong 53.

Trait	TC XD23	TC XD53	YL XD23	YL XD53	qG (TC)	qG (YL)
Protein content (%)	15.15 ± 0.10	14.02 ± 0.07	13.57 ± 0.23	12.50 ± 0.23	0.001	0.008
Wet gluten (%)	30.58 ± 0.17	31.49 ± 0.28	26.86 ± 0.51	26.13 ± 0.09	0.020	0.091
Gluten index (%)	99.19 ± 0.23	94.91 ± 0.90	96.51 ± 1.54	96.33 ± 0.64	0.008	0.835
Stability time (min)	23.23 ± 2.56	10.43 ± 0.42	13.43 ± 1.72	7.50 ± 0.35	0.001	0.046
Development time (min)	47.60 ± 1.49	5.47 ± 0.25	4.63 ± 1.86	5.37 ± 0.51	<0.001	0.475
Extensograph energy (cm^2)	178.97 ± 15.63	90.20 ± 2.76	79.90 ± 3.47	60.30 ± 0.50	0.001	0.110
Resistance (BU)	429.33 ± 17.97	283.67 ± 14.25	238.17 ± 15.31	201.83 ± 5.84	0.001	0.110
Extensibility (mm)	184.60 ± 6.97	163.60 ± 8.87	178.10 ± 6.13	168.33 ± 6.59	0.028	0.256

Mean ± SD of three field plots per cultivar–site group. TC, Tacheng; YL, Yili. qG (TC) and qG (YL) are blocked-model cultivar contrasts (Xindong 23 minus Xindong 53), BH-adjusted across eight traits within each site. Protein content is on a dry basis.

Table 2. Quality index differences between Tacheng and Yili within each cultivar.

Trait	XD23 Δ	95% CI	q	XD53 Δ	95% CI	q
Protein content (%)	1.59	1.25, 1.93	<0.001	1.51	1.17, 1.85	<0.001
Wet gluten (%)	3.71	3.06, 4.36	<0.001	5.36	4.71, 6.00	<0.001
Gluten index (%)	2.68	0.48, 4.89	0.032	−1.42	−3.63, 0.78	0.196
Stability time (min)	9.80	6.07, 13.53	0.003	2.93	−0.80, 6.66	0.151
Development time (min)	42.97	40.72, 45.21	<0.001	0.10	−2.15, 2.35	0.908
Extensograph energy (cm^2)	99.07	78.28, 119.85	<0.001	29.90	9.11, 50.69	0.032
Resistance (BU)	191.17	150.38, 231.95	<0.001	81.83	41.05, 122.62	0.014
Extensibility (mm)	6.50	−10.81, 23.81	0.356	−4.73	−22.04, 12.57	0.560

Values are Tacheng minus Yili (Δ) in the trait units, with unadjusted 95% model confidence intervals and BH q values across eight traits for each cultivar-specific contrast. Each cultivar–site group contains three field plots. Estimates account for blocks nested within site; residual df = 4.

Table 3. Marginal main effects and genotype-by-site interactions for eight quality traits.

Trait	qG	qSite	G × Site ΔΔ	95% CI	Pinteraction	Qinteraction
Protein content (%)	<0.001	<0.001	0.07	−0.41, 0.55	0.694	0.694
Wet gluten (%)	0.628	<0.001	−1.65	−2.56, −0.73	0.008	0.015
Gluten index (%)	0.022	0.372	4.11	0.99, 7.23	0.022	0.030
Stability time (min)	0.001	0.003	6.87	1.59, 12.14	0.022	0.030
Development time (min)	<0.001	<0.001	42.87	39.69, 46.04	<0.001	<0.001
Extensograph energy (cm^2)	0.001	<0.001	69.17	39.77, 98.57	0.003	0.011
Resistance (BU)	0.001	<0.001	109.33	51.66, 167.01	0.006	0.015
Extensibility (mm)	0.029	0.851	11.23	−13.24, 35.71	0.272	0.310

qG and qSite refer to marginal genotype and site effects. The interaction estimate $\Delta\Delta = (TC - YL)XD23 - (TC - YL)XD53$, in trait units. All q values are BH-adjusted across eight traits within the corresponding contrast. Confidence intervals are unadjusted 95% model intervals; residual df = 4. Complete effects and sensitivity results are in Table S1.

2.3. Transcriptome Sequencing and Bioinformatic Analysis

Both focal cultivars flowered on 15 May 2025 in Yili and 27 May in Tacheng. Developing grains were sampled at nominal 10, 20 and 30 DAA: 25 May, 5 June and 15 June in Yili (actual 10, 21 and 31 DAA), and 6, 16 and 26 June in Tacheng (actual 10, 20 and 30 DAA). At each stage, at least 50 grains from the middle of the main spikes of representative, disease-free plants were collected within each field plot. Grains within a plot were subsamples; the three blocks provided biological replication. RNA and protein measurements came from the same plot and stage, giving 36 samples from 12 independent plots. Samples were immediately frozen in liquid nitrogen for 10 min and stored at −80 °C.

Total RNA extraction and transcriptome sequencing were performed by Tianjin Jizhi Gene Technology Co., Ltd. (Tianjin, China). Poly(A)-enriched libraries were prepared using the Hieff NGS Ultima Dual-mode RNA Library Prep Kit (Premixed version; Yeasen), with MGI adapters and single-strand circularization, and sequenced on the DNBSEQ-T7 platform. Low-quality and adapter-containing reads were filtered with fastp (v0.23.4) [32].

Clean reads were mapped to the Chinese Spring IWGSC RefSeq v1.1 reference using HISAT2 (v0.23.4) [33], with transcript assembly and FPKM summaries provided by StringTie (v2.2.0) [34]. Unnormalized integer gene counts were used for differential testing with the DESeq2 framework through PyDESeq2 0.5.4 [35]. Each nominal stage was analysed separately with site, genotype, genotype × site and block nested within site as fixed effects. Genes with counts ≥10 in at least three stage-specific samples were retained. Wald contrasts used Cook's filtering; non-converged coefficients were excluded, and BH correction was applied to finite *p* values within each stage–contrast family. Site and within-site cultivar contrasts required $q < 0.05$ and $|\log2 \text{ fold change}| \geq 1$; interaction tests required $q < 0.05$ only. FPKM was used for descriptive PCA and heatmaps [36], not DESeq2 inference. Cross-stage interaction BH results are supplied as sensitivity analyses in Dataset S1.

2.4. Weighted Gene Co-Expression Network Analysis (WGCNA)

Weighted gene co-expression network analysis was summarized from the archived gene-membership, module-eigengene, kME and within-module connectivity outputs for 36 samples. The supplied soft-power plot reports $\beta = 16$ and a scale-free fit cutoff of 0.85. The archived clustering dendrogram is retained in Figure 1a, and group mean supplied eigengenes are shown in Figure 1b. The red and yellow candidates were ranked by descending supplied kWithin, with ties resolved by gene ID; the first 20 genes were reported with kME and functional annotations (Table S4). The analysis provides exploratory co-expression associations. Available outputs and the limits of recovering the original network-construction settings are documented in Supplementary Methods.

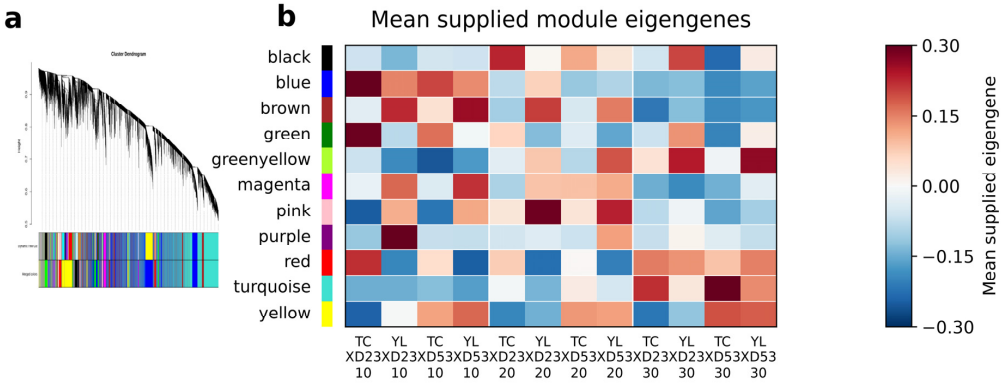


Figure 1. Weighted gene co-expression network summaries. (**a**) Archived hierarchical clustering dendrogram retained from the submitted figure; grey denotes unassigned genes. Module membership records 11 assigned modules plus grey. (**b**) Mean supplied module eigengenes for each cultivar–site–stage group (three field blocks per group). Colour indicates eigengene values, rather than module–quality correlations or significance. TC, Tacheng; YL, Yili. Module membership, connectivity, kME and eigengenes are supplied in Table S4 and its associated dataset.

2.5. Proteome Sequencing and Bioinformatic Analysis

To characterize storage-protein abundance patterns during wheat grain filling, quantitative proteomic analysis was performed on grain samples collected at key filling stages. The sampling time points and procedures were consistent with those used for transcriptomic sequencing. All sample preparation and proteomic assays were conducted by Tianjin Jizhi Gene Technology Co., Ltd. Briefly, grain samples were fully ground into fine powder in liquid nitrogen, and total proteins were extracted using the phenol extraction method. Protein quantification was performed via the BCA assay for concentration calibration. After reduction, alkylation, and trypsin digestion, the resulting peptides were analysed by label-free data-independent acquisition (DIA), using a Vanquish neo LC system coupled to an Astral mass spectrometer (Thermo Scientific), as specified in the project laboratory report.

Raw MS files were processed in Spectronaut 19.0.240604.62635 with the built-in Pulsar engine against uniprotkb_Triticum_aestivum_id_4565_2025_04_27.fasta. Search parameters were trypsin with up to two missed cleavages, fixed carbamidomethylation of cysteine, variable methionine oxidation and protein N-terminal acetylation, and 20 ppm precursor and fragment tolerances. The vendor report specifies 1% FDR at PSM and peptide levels; a separate protein-identification FDR is not inferred. For differential analysis, non-positive abundances were treated as missing, positive values log2-transformed and sample medians aligned across the 36 focal samples. No missing abundance was imputed. Descriptive PCA used 6997 proteins complete across all 36 samples, centred by protein without variance scaling. Pearson sample correlations used these same profiles; clustering used average linkage and distance 1 – r. At each nominal stage, proteins complete across its 12 samples

were tested with the same blocked genotype-by-site design as the quality analysis (residual df = 4). Two-sided t contrasts and BH correction were applied within each stage–contrast family. Site and within-site cultivar contrasts required $q < 0.05$ and $|\log2 \text{ fold change}| \geq \log2(1.5)$ [37]; interactions required $q < 0.05$ only. Cross-stage interaction correction and missingness summaries are provided in Dataset S1. Identification FDR and differential-analysis FDR concern different testing stages.

2.6. Complementary Quantitative Real-Time PCR Analysis

Quantitative real-time PCR (qRT-PCR) was used as a complementary measurement of selected transcript patterns during grain filling. Total RNA was extracted using Trizol reagent (Invitrogen, Carlsbad, CA, USA), and the first-strand cDNA was synthesized via reverse transcription using the PrimeScript™ RT Reagent Kit (TaKaRa, Shiga, Japan) following the manufacturer's protocols. The reverse transcription reaction was performed at 37 °C for 15 min, followed by 85 °C for 5 s for enzyme inactivation. The synthesized cDNA was stored at −20 °C for subsequent use.

Primer sequences retained from the submitted protocol are provided in Table S6. Reactions used TB Green Premix Ex Taq II in a 20 µL volume, as specified in the submitted protocol. Single-well target and matched *TaActin* Cq values were taken from the latest Bio-Rad CFX software exports. Each cultivar–site–stage group contained three biological samples from blocks I–III of the same plots used for omics; no independent field-validation cohort or technical triplicate is claimed. ΔCt was calculated as target Cq minus its assay-specific matched *Actin* Cq. At each stage, −ΔCt was fitted with the blocked genotype-by-site model; site contrasts were BH-adjusted across 48 comparisons and interactions across 24, with unadjusted 95% confidence intervals. Figure 2 reports cycle effects. Optional 2^(−ΔΔCt) ratios in Table S7 assume equal 100% efficiencies for target and reference [38]. *Actin* diagnostics, raw Cq pairs and source-curve checks are supplied, but reference stability, efficiency and amplicon specificity were not established. The single-well results are interpreted conditionally and do not validate the proteome.

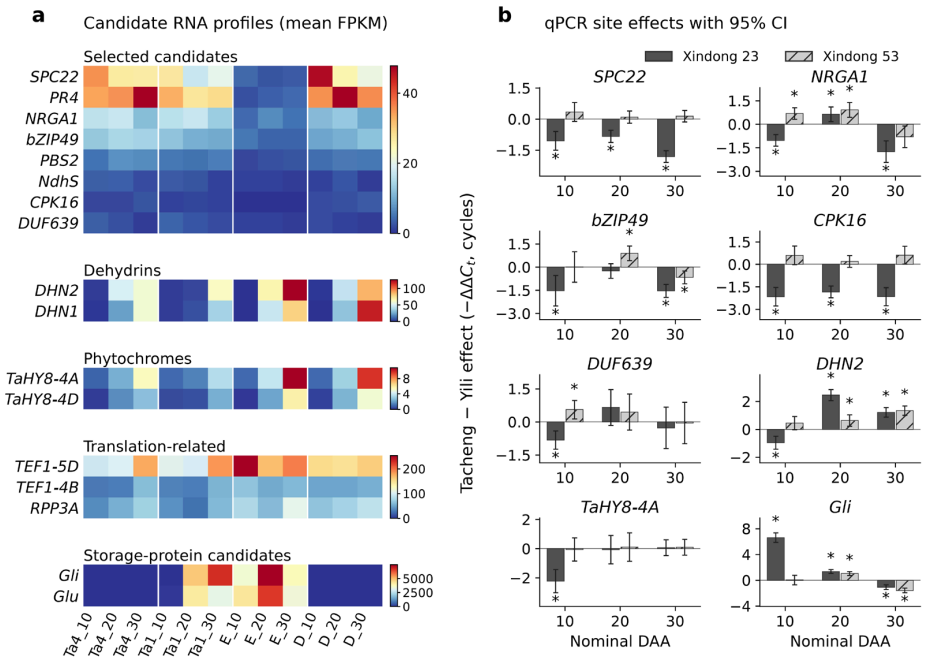


Figure 2. Candidate RNA profiles and complementary qRT-PCR site contrasts. (**a**) Seventeen submitted candidates in five groups; colours show arithmetic mean FPKM across three field blocks. Each group has its own untransformed colour scale. Ta4/Ta1 denote Xindong 53/23 in Yili, and E/D denote

Xindong 23/53 in Tacheng. (**b**) Eight target-specific panels of blocked-model Tacheng-minus-Yili effects on −ΔCt, shown as −ΔΔCt in cycles. Bars are estimates, and error bars are unadjusted 95% t confidence intervals (residual df = 4). Positive effects indicate higher target expression relative to matched *Actin* in Tacheng, conditional on reference and assay performance; zero denotes no estimated site difference. Asterisks indicate BH $q < 0.05$ across 48 site contrasts. Each group contains three biological plots with single-well measurements. Stages are nominal DAA. Raw Cq values and exact statistics are in Table S7; Figure S4 shows the same effects and intervals.

2.7. Functional Enrichment and Direct Transcript–Protein Integration

GO and KEGG enrichment was recalculated from the blocked-model differential lists using one-sided hypergeometric tests in SciPy, with BH correction through statsmodels. Backgrounds were the stage- and contrast-specific tested molecules with annotations in the relevant layer and library; each GO ontology was treated separately. RNA GO mappings used archived UniProt annotations and unique IWGSC cross-references, RNA KEGG used supplied KO annotations linked to archived official pathway mappings, and proteins used exact UniProt accessions. GO is_a and part_of ancestors were included, excluding roots. Terms with 10–1000 background members were tested, including zero-hit terms. The primary BH family was layer × stage × contrast × direction × library; correction across all contrasts and directions within each layer/library was retained as sensitivity. Enrichment is an annotation-level association and does not measure pathway activity [39,40]. Full inputs, background IDs, coverage and versions are in Dataset S2.

Direct gene–protein matching used archived UniProt EnsemblPlants cross-references. A protein entry was retained only if it mapped to one compatible IWGSC gene, that gene mapped uniquely to one accession, and the entry was not an ambiguous multi-accession group. RNA and protein site-effect tables were joined by these IDs, retaining all finite matched effects for Pearson and Spearman correlations, sign concordance and dual-threshold summaries. Descriptive abundance correlations used log2(FPKM +1) and normalized log2 protein abundance across matched samples, with additional residual correlations after accounting for plot and cultivar–site–stage cells. The 36 repeated-stage samples represent 12 field plots. GO intersections were computed independently from significant ontology IDs in the two layers, rather than substituted for direct molecular matching (Table S5).

3. Results

3.1. Effects of Ecological Environments on Wheat Grain Morphology and Quality Traits

Field trials were carried out in two typical ecological regions (Tacheng and Yili) to explore site-associated differences in grain development and quality formation in wheat. The morphological characteristics of mature grains from the two cultivars are presented in Figure 3. Within each site, Xindong 53 exhibited higher mean grain width and 1000-kernel weight than Xindong 23 (Table S3). Grains produced in Tacheng also had greater mean width and 1000-kernel weight than those from Yili. For Xindong 23, mean width was 2.74 versus 2.52 mm and 1000-kernel weight was 42.33 versus 33.09 g; the corresponding values for Xindong 53 were 3.04 versus 2.55 mm and 47.89 versus 34.55 g (Table S3). Figure 3a,b illustrates grain appearance and transverse sections; colour and vitreous-kernel proportions were not quantified.

To clarify the independent and interactive effects of genotype and environment on wheat processing quality, we systematically determined core grain and flour quality indices of the two cultivars (Table S1). In terms of cultivar differences, Table 1 shows higher protein content and longer dough stability time in Xindong 23 than in Xindong 53 at both Tacheng and Yili under the blocked factorial model. Specifically, in both locations, the protein content of Xindong 23 was approximately 8% higher than that of Xindong 53, and its dough stability

time was significantly longer. Meanwhile, Xindong 23 had higher extensograph energy and extensograph resistance, with significant cultivar differences in Tacheng but not Yili after BH correction. In Tacheng, Xindong 23 had lower wet gluten content and higher extensibility; neither cultivar contrast was significant in Yili. However, dough development time and gluten index presented a location-dependent divergence: higher values in Xindong 23 were observed in Tacheng, whereas the cultivar contrasts were not significant under Yili cultivation conditions.

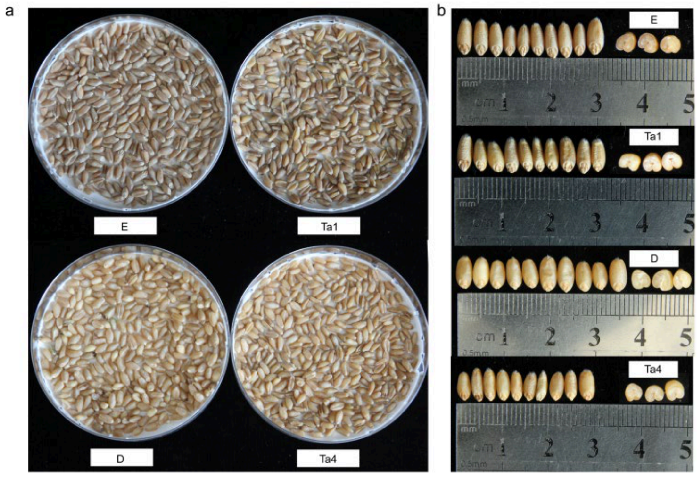


Figure 3. Grain phenotypic characteristics of Xindong 23 and Xindong 53 cultivated in Tacheng and Yili. (**a**) The overall grain morphology of two wheat cultivars harvested from Tacheng and Yili; (**b**) grain width (**left**) and transverse section structure (**right**). Sample codes: E, Xindong 23 in Tacheng; Ta1, Xindong 23 in Yili; D, Xindong 53 in Tacheng; Ta4, Xindong 53 in Yili. Scale bars represent millimetres (mm), illustrating differences in grain width and plumpness. Photographs are descriptive; plot-level dimensions and 1000-kernel weight are provided in Table S3.

Comparative analysis of quality indicators between the two ecological environments revealed significant site-associated effects on wheat quality (Table 2). Compared with plants grown in Yili, both Xindong 23 and Xindong 53 from Tacheng attained significantly higher protein content, wet gluten content, extensograph energy and extensograph resistance. The site contrast for dough stability time was significant in Xindong 23 (9.80 min; $q = 0.003$), but not in Xindong 53 (2.93 min; $q = 0.151$). Gluten index differed between sites in Xindong 23 only, while neither cultivar showed a significant site effect on extensibility. Notably, dough development time showed a pronounced site difference in Xindong 23, while the site contrast was not significant in Xindong 53.

Formal genotype-by-site interactions were significant for wet gluten content, gluten index, dough stability time, dough development time, extensograph energy and extensograph resistance (Table 3). The stability-time interaction was 6.87 min (95% CI 1.59–12.14; $q = 0.030$), indicating a larger Tacheng-minus-Yili difference in Xindong 23. Protein content and extensibility did not show significant interactions.

The coefficient of variation (CV) of quality traits was calculated to describe within-site variation among the three field blocks of each cultivar. Xindong 53 exhibited an average CV of 3.07%, which was markedly lower than the 6.54% observed for Xindong 23. Specifically, the CV value of dough stability time in Xindong 53 was approximately 36% of that in Xindong 23. Similarly, the CV values of dough development time and extensograph energy in Xindong 53 were approximately one-third of those in Xindong 23. For other traits, including protein content, wet gluten content, gluten index, and extensograph resistance, Xindong 23 also exhibited slightly higher variation than Xindong 53 among blocks within the two sites (Figure 4). Each trait CV is the mean of the two site-specific block CVs, and

the overall CV is the arithmetic mean across the eight traits. Cultivar-specific site responses are evaluated separately by the factorial model (Table 3).

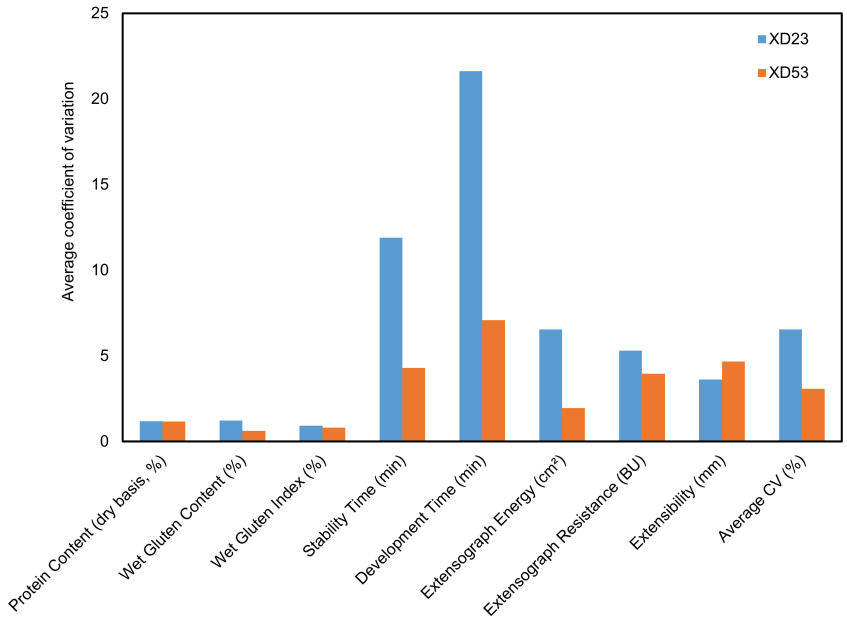


Figure 4. Coefficient of variation (CV) comparison of quality indices between XD23 and XD53 within the two regions. The horizontal axis presents key quality traits. The vertical axis indicates the average coefficient of variation (CV, %), calculated within each site from three field blocks and then averaged over the two sites. Blue bars represent XD23, and orange bars represent XD53. The final bars are arithmetic averages across the eight quality traits; this is a descriptive measure of within-site block dispersion.

3.2. Transcriptional Response Characteristics of Wheat Grains Under Heterogeneous Environments

To characterize the transcriptional responses associated with site-specific quality differentiation in wheat, transcriptomic analysis was performed on grains of Xindong 23 and Xindong 53 at three nominal grain-filling stages (10, 20, and 30 DAA). Principal component analysis (PCA) of the 2000 most variable log2(FPKM + 1) profiles showed that samples were clustered primarily by grain developmental stage, with PC1 and PC2 explaining 54.58% and 17.94% of expression variation (Figure 5a). Differential gene statistics revealed that, at the early (10 DAA) and middle (20 DAA) grain-filling stages, substantially more DEGs were identified in Xindong 23 between the two ecological sites (E_10 vs. Ta1_10, E_20 vs. Ta1_20) than in cultivar comparisons within the same environment (E_10 vs. D_10, E_20 vs. D_20, Ta1_10 vs. Ta4_10, Ta1_20 vs. Ta4_20). The blocked model identified 11,139, 5823 and 2235 site-associated DEGs in Xindong 23 at nominal 10, 20 and 30 DAA, respectively, compared with 2812, 622 and 2535 in Xindong 53. Genotype-by-site interaction tests identified 6821, 244 and 193 genes at these stages (Figure 5b; Dataset S1).

Volcano plot analysis revealed genes with both positive and negative site-associated effects (Figure 5c; Figure S3). In Xindong 23, more DEGs had lower expression in Tacheng than in Yili at each nominal stage. These transcriptional differences reflect the overall regional site contrast, which combines multiple environmental conditions.

GO enrichment analysis further showed stage-specific functional differences among the site-associated DEGs (Figure 6a,b). In Xindong 23, prominent terms included response to oxidative stress, secondary-metabolite biosynthesis and response to water, with ribosome biogenesis and rRNA processing at middle filling. In comparison, Xindong 53 showed enrichment involving photosynthesis and light harvesting at early and late filling, and protein folding at middle filling.

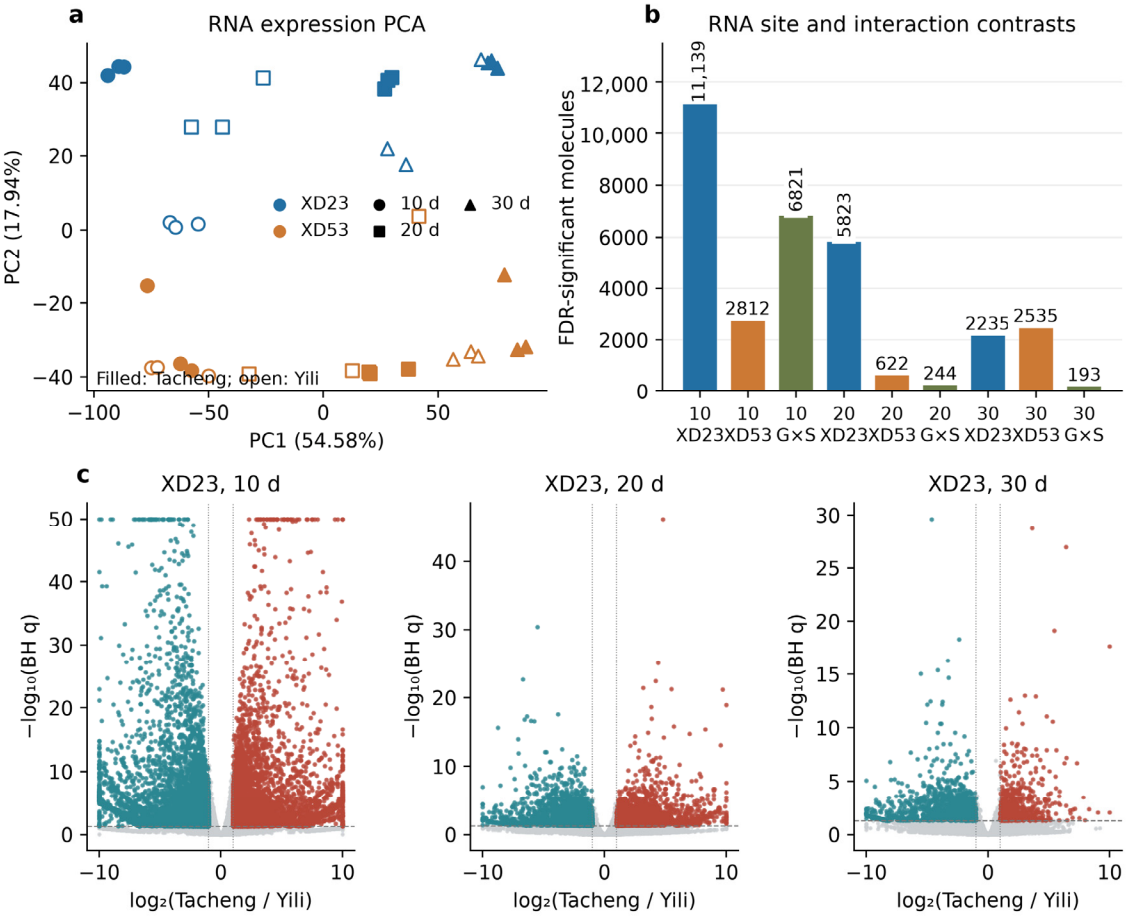


Figure 5. Transcriptomic profiles and blocked differential analysis. (**a**) PCA of 36 samples using the 2000 most variable log2(FPKM + 1) profiles. Colour identifies cultivar; filled/open symbols denote Tacheng/Yili, and shapes denote nominal stage. (**b**) Significant site contrasts in each cultivar and genotype-by-site interactions (G × S). (**c**) Xindong 23 site-contrast volcano plots at nominal 10, 20 and 30 DAA; corresponding Xindong 53 plots are in Figure S3. Red/teal denote positive/negative significant effects, and grey denotes other tested genes. The x-axis is log2(Tacheng/Yili), clipped at ±10 for display; the y-axis is −log10(BH q). Site calls use $q < 0.05$ and $|\log2 \text{ fold change}| \geq 1$.

KEGG analysis demonstrated that site-associated DEGs of Xindong 23 were enriched in starch and sucrose metabolism, phenylpropanoid biosynthesis and protein processing in the endoplasmic reticulum at early filling (Figure 6c). The ER-processing enrichment had $q = 2.52 \times 10^{-4}$. In Xindong 53, photosynthesis–antenna proteins were enriched at early and late filling, while protein processing in the endoplasmic reticulum was enriched at middle and late filling (Figure 6d). These results indicate cultivar- and stage-dependent enrichment of protein-processing and metabolic pathways. At late filling, the Xindong 23 site-associated DEG set was also enriched in nitrogen metabolism ($q = 5.08 \times 10^{-4}$; Figure 6c; Dataset S2).

To explore biological processes associated with grain quality formation, the two largest Xindong 23 site-associated DEG sets (E_10 vs. Ta1_10 and E_20 vs. Ta1_20) were examined in further detail. The ribosome pathway was enriched at middle filling ($q = 5.19 \times 10^{-29}$), while the formal interaction-associated gene set also showed ER-processing enrichment at nominal 10 DAA ($q = 2.74 \times 10^{-13}$; Dataset S2). Interaction effects describe differences between cultivar-specific site responses; their distributions are shown in Figure S1.

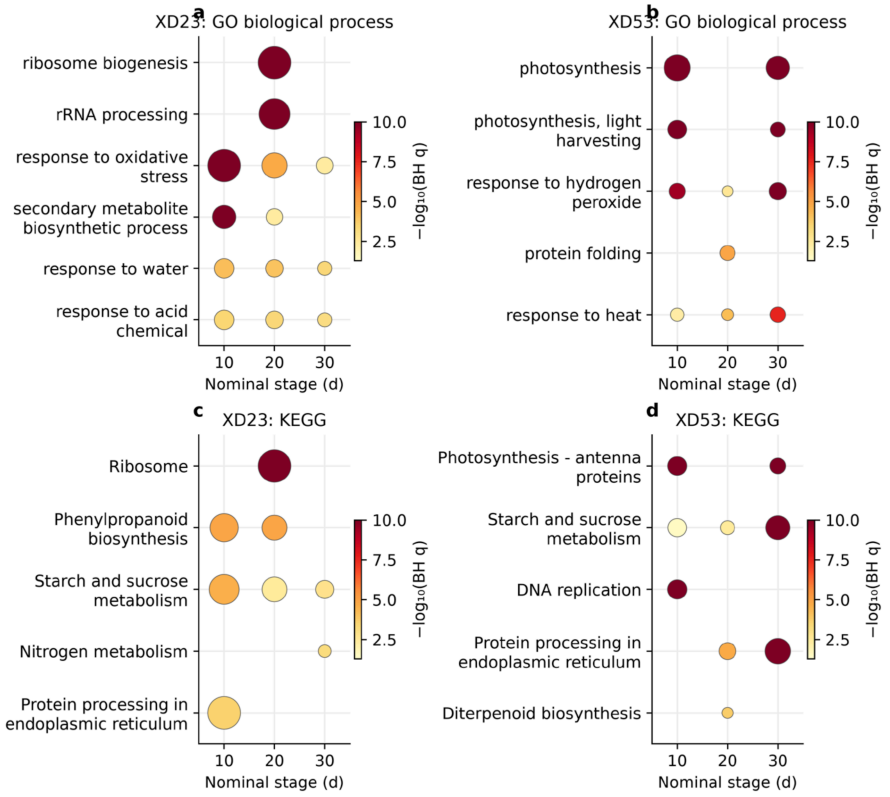


Figure 6. Stage-specific GO and KEGG enrichment of site-associated DEGs. (**a**,**b**) Selected GO biological-process terms for Xindong 23 and Xindong 53; (**c**,**d**) selected KEGG pathways for the same cultivars. Columns denote nominal 10, 20 and 30 DAA. Bubble area represents the number of annotated differential genes, and colour represents −log10(BH q), capped at 10 for display. Terms were selected from the two lowest-q terms per stage; the early Xindong 23 ER-processing pathway was additionally retained for the study question. Only within-family BH q < 0.05 results are plotted. Exact backgrounds, all directions, all GO ontologies and full results are provided in Supplementary Dataset S2.

3.3. Gene Co-Expression Network Characteristics

The archived co-expression outputs contained 36,181 genes across 36 samples, with a reported soft threshold of $\beta = 16$ and scale-free fit cutoff $R^2 = 0.85$. Module partitioning recorded 11 assigned modules plus the unassigned grey group; assigned module sizes ranged from 141 to 12,282 genes (Figure 1a; Table S4). Group mean eigengenes showed higher red-module values in Tacheng than in Yili at early and middle filling in both cultivars. In comparison, the yellow module generally had higher eigengene values in Xindong 53 than in Xindong 23 (Figure 1b).

Functional annotation of the 20 most highly connected genes in the site-associated red module included ribosomal protein genes, translation initiation factor 2A and elongation factor 1-alpha. These candidates exhibit high intra-module connectivity and provide translation-related co-expression associations. Detailed functional annotations and expression profiles of these candidate genes are summarized in Table S4.

In contrast, the 20 most highly connected genes in the cultivar-associated yellow module covered a broader spectrum of functional annotations (Table S4). The red and yellow candidates were ranked by supplied within-module connectivity (kWithin), with module membership (kME) reported alongside annotations. Among the qRT-PCR targets, *SPC22* and *bZIP49* mapped to yellow and *NRGA1* to pink, but none was in these top-20 rankings; candidate selection therefore also drew on transcript contrasts and functional annotations.

3.4. Proteomic Responses of Wheat Grains to Heterogeneous Environments During Grain Filling

To characterize genotype-specific differences in grain protein abundance in wheat under distinct ecological conditions, label-free DIA proteomic profiling was performed on grain samples collected throughout the grain-filling period. Principal component analysis (PCA) (Figure 7a) and correlation heatmap analysis (Figure 7b) summarized variation among samples based on 6997 proteins with complete abundance records across the 36 focal samples. PCA showed that PC1 and PC2 explained 53.23% and 11.22% of the proteomic variation, respectively, describing protein-abundance differences in wheat grains during grain filling. Differential analysis identified the greatest number of site-associated proteins in Xindong 23 at the early grain-filling stage (nominal 10 DAA).

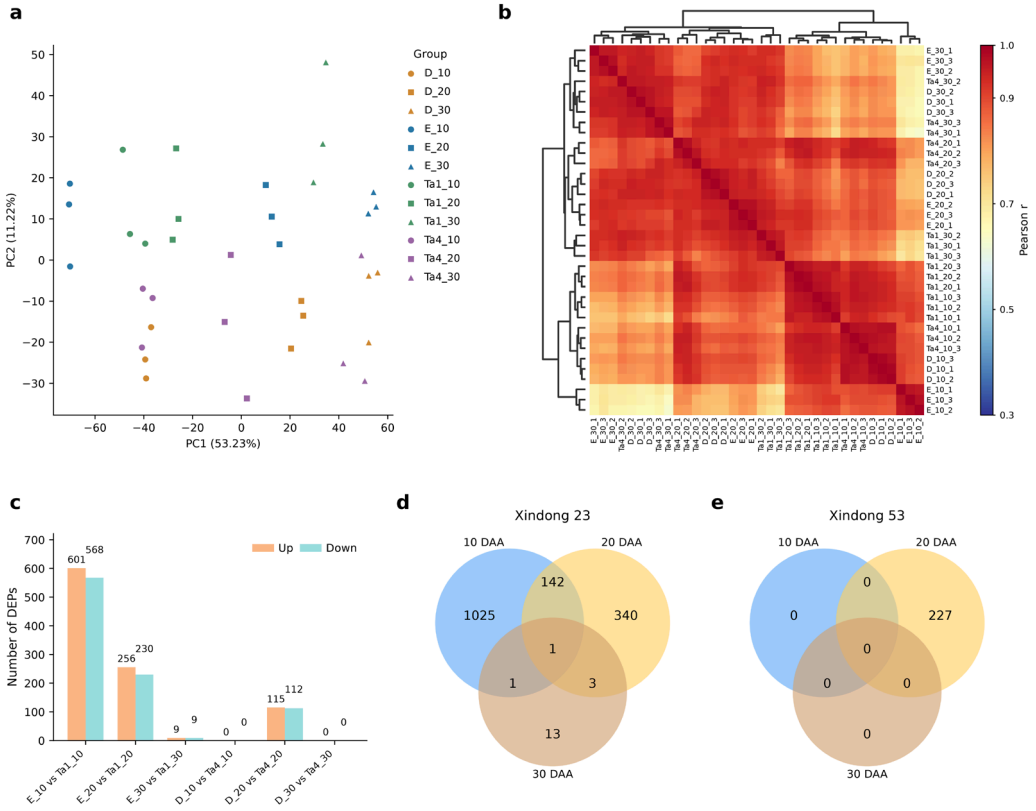


Figure 7. Analysis of DEPs in wheat grains during grain filling. (**a**) PCA of 6997 complete, median-normalized log2 protein profiles across 36 samples. (**b**) Pearson sample correlations with average-linkage clustering using distance 1 – r. (**c**) Up-regulated (orange) and down-regulated (light blue) DEPs in Tacheng relative to Yili. Site contrasts require BH $q < 0.05$ and $|\log2 \text{ fold change}| \geq \log2(1.5)$. (**d**,**e**) Venn diagrams of stage-overlapping DEPs in Xindong 23 and Xindong 53, respectively; counts are exact and circle areas are schematic. E/D denote Xindong 23/53 in Tacheng; Ta1/Ta4 denote Xindong 23/53 in Yili. Stages are nominal DAA labels; final suffixes 1–3 denote field blocks. Interaction results are in Figure S1 and Dataset S1.

Distinct genotypic differences in environmental responsiveness were observed between the two cultivars. Xindong 23 exhibited more site-associated differential proteins at early grain filling, whereas Xindong 53 displayed fewer proteins passing the corresponding FDR thresholds. The correlation heatmap provides descriptive context for these protein-abundance profiles (Figure 7b).

Statistical analysis of DEPs revealed significant stage- and genotype-specific variations in environmental response intensity. For Xindong 23, the numbers of environment-responsive DEPs at 10, 20, and 30 DAA were 1169, 486 and 18, respectively, exhibiting a dynamic pattern of strong response at the early filling stage followed by a gradual decline.

In contrast, Xindong 53 possessed substantially fewer DEPs at the corresponding stages (0, 227 and 0, respectively) (Figure 7c), under the same blocked model and FDR thresholds. Venn analysis of stage-overlapping DEPs across the entire filling period identified one site-associated DEP in Xindong 23 and none in Xindong 53 passing thresholds at all three stages (Figure 7d,e). Formal genotype-by-site interaction tests identified 83 proteins at early filling and none at the other two stages (Dataset S1; Figure S1).

Functional annotation and enrichment of the updated DEP sets were used to examine protein responses across grain filling. Full stage-specific differential lists and GO/KEGG results are supplied in Datasets S1 and S2, respectively. These outputs retain the complete results beyond the selected terms displayed in Figure 8.

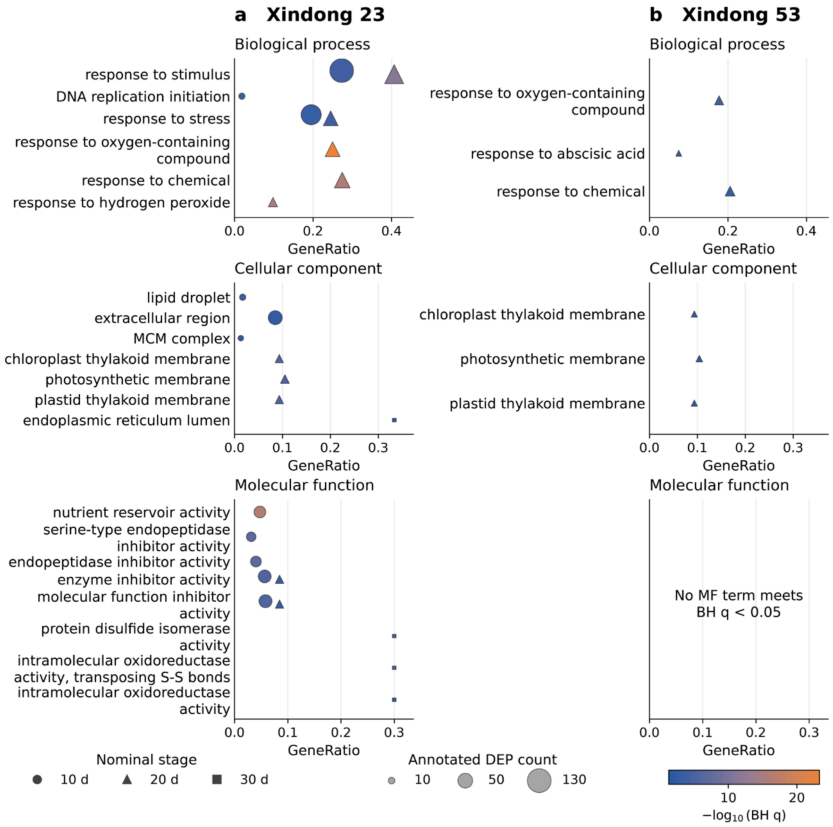


Figure 8. Stage-specific GO enrichment of site-associated DEPs. (**a**) Xindong 23; (**b**) Xindong 53. Rows show biological process, cellular component and molecular function. GeneRatio is the number of DEP hits divided by the number of DEPs annotated in that ontology for the corresponding contrast. Marker area represents hit count; circles, triangles and squares denote nominal 10, 20 and 30 DAA. Colour represents −log10(BH q). The three lowest-q terms per stage and ontology were selected (ties by GO ID), with all significant occurrences of selected terms shown. Only within-family BH $q < 0.05$ results are plotted. Xindong 53 had no significant molecular-function term. Full results and backgrounds are in Dataset S2.

GO enrichment analysis revealed differences in the stage-specific site-associated DEP sets between the two cultivars. Xindong 23 DEPs were enriched in response to stimulus and DNA replication initiation at early filling, and in response to oxygen-containing compounds and response to chemical at middle filling (Figure 8a). In comparison, Xindong 53 showed middle-stage enrichment of response to oxygen-containing compounds and response to abscisic acid (Figure 8b). Additional enriched annotations in Xindong 23 included nutrient reservoir activity at early filling, and endoplasmic reticulum lumen and protein disulfide isomerase activity at late filling; each of these late-stage terms contained three

DEP hits (Figure 8a). Complete enrichment results and tested backgrounds are provided in Dataset S2.

3.5. Integrative Transcriptomic and Proteomic Analysis of Site-Associated Quality Differences in Wheat

By integrating the transcriptomic and proteomic data of grains collected from the two ecological regions, we screened common significantly enriched GO IDs at each grain-filling stage (Table S5). Under the updated FDR thresholds and annotation backgrounds, Xindong 23 had 11 and 24 shared RNA–protein GO terms at early and middle filling, respectively, and none at late filling. No shared term passed both layers in Xindong 53. These annotation-level overlaps were complemented by direct gene-to-protein matching.

Direct matching yielded 8532, 7353 and 6271 unique gene–protein pairs with finite site effects at nominal 10, 20 and 30 DAA, respectively. In Xindong 23, Pearson correlations between matched transcript and protein log2 site effects were 0.283, 0.383 and 0.073; the corresponding values for Xindong 53 were 0.090, 0.125 and 0.113 (Figure S2; Table S5). At early and middle filling, 237 and 131 Xindong 23 pairs passed both layers, of which 215 and 129 agreed in direction, supporting partial, stage-dependent cross-layer concordance.

Distinct site-associated responses were also observed among candidate storage-protein annotations. For example, the omega-gliadin pair *TraesCS1D02G000582*/A0A3B5ZM30 had positive RNA and protein site effects in Xindong 23 at middle filling (log2 fold changes 2.22 and 0.99, respectively), passing both thresholds. The corresponding RNA and protein site contrasts did not pass the respective differential thresholds in Xindong 53 (Table S5). This matched candidate provides a molecular association for further investigation of grain quality; glutenin/gliadin composition and its functional contribution require targeted measurement.

3.6. Complementary qRT-PCR Analysis

To further characterize the spatiotemporal expression patterns of candidate quality- and stress-responsive genes under contrasting ecological conditions, we selected eight candidate genes associated with stress responses and protein-related functions for complementary qRT-PCR analysis (Table S6). Gene selection drew on transcript contrasts and functional annotations; available WGCNA membership is reported separately in Table S4.

By integrating transcriptomic heatmaps with complementary qRT-PCR measurements, we examined candidate transcriptional profiles across ecological sites, wheat genotypes and post-anthesis developmental stages (Figure 2a,b; Table S7). The RNA heatmaps retain the 17 submitted candidates in their original groups, with gene IDs and group means checked against the 36-sample expression matrix (Figure 2a; Table S7). The eight qRT-PCR targets included *SPC22*, *NRGA1*, *bZIP49*, *CPK16*, *DUF639*, *DHN2*, *TaHY8-4A* and a gliadin candidate (Table S6). Using the latest single-well Cq exports, 28 of 48 cultivar-specific site contrasts and 14 of 24 interactions passed BH $q < 0.05$; site-effect directions agreed with RNA estimates in 30 of 48 comparisons. These complementary transcript results are conditional on the matched *TaActin* reference and assay performance; three biological samples per group came from the same field plots as the omics analyses.

Together, the phenotypic, transcriptomic, co-expression and proteomic results in Sections 2.1–2.5 are synthesized in Figure 9. The scheme relates cultivar-specific molecular responses to observed quality differences as a working hypothesis.

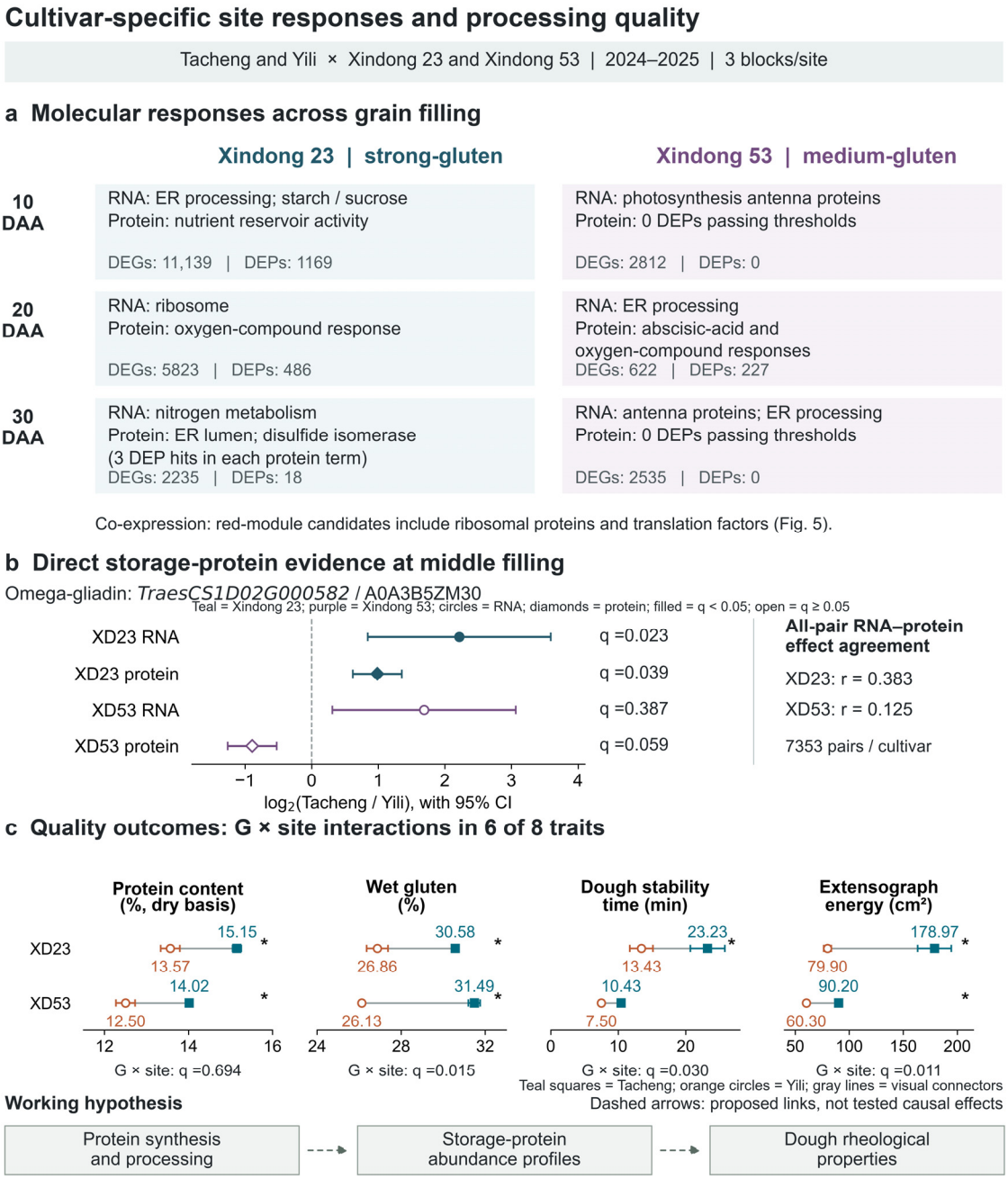


Figure 9. Synthesis of cultivar-specific site responses and wheat processing quality. (**a**) Representative RNA/protein enrichment and DEG/DEP counts for Tacheng versus Yili. Enrichment uses combined up- and down-regulated sets (within-family BH $q < 0.05$), without inferring pathway activation. ER, endoplasmic reticulum; stages denote nominal DAA (actual Yili: 10/21/31; Tacheng: 10/20/30). (**b**) Matched omega-gliadin at 20 DAA: log2(Tacheng/Yili) effects, unadjusted 95% intervals (RNA Wald; protein t, df = 4), and layer-specific BH q. Filled markers pass differential thresholds; open markers do not. Pearson r uses all 7353 finite pairs per cultivar. (**c**) Four representative traits: dry-basis protein content, wet gluten, dough stability time and extensograph energy (mean ± SD; three plots per cultivar–site group). Lines connect site means. Stars mark site contrasts (BH $q < 0.05$); interaction q values appear below. Six of the eight quality traits showed genotype × site interactions at BH $q < 0.05$, using eight-trait correction families (Tables 2 and 3). Dashed arrows denote a working hypothesis linking protein processes and quality. Glutenin/gliadin proportions were not measured. Sources: Tables S3–S5 and Datasets S1 and S2.

4. Discussion

Wheat quality is a complex quantitative trait cooperatively governed by genotype (G), environment (E), and their interactive effects (G × E) [41]. The period from flowering to maturity is critical for determining grain yield and quality, during which environmental factors such as disease pressure, light availability, and moisture supply exert significant influences on final grain quality and yield [42,43]. In the present study, two winter wheat cultivars with contrasting gluten characteristics were cultivated in two ecologically divergent regions (Yili and Tacheng), during one growing season, and significant genotypic differences in processing quality traits were detected. Both cultivars exhibited higher protein content, wet gluten content, extensograph energy and extensograph resistance under Tacheng conditions. Notably, Xindong 53 showed smaller site differences in several rheological traits, whereas Xindong 23 showed pronounced site-associated variation in key quality traits. Formal interactions for six of eight quality traits support distinct cultivar responses within this trial and highlight the value of testing cultivar–environment matching across additional sites and seasons.

The environment-dependent quality divergence may involve metabolic trade-offs between stress defence and storage substance accumulation. Limited soil moisture increases wheat grain protein content, a phenomenon attributed to over-accumulated nitrogen compounds and reduced carbohydrate partitioning to storage reserves, whereas excessive humidity adversely affects the polymerization of storage proteins [44]. In this study, stress-response transcript and protein annotations differed between the sites, including water- and oxidative-stress-related terms. Such patterns are compatible with altered resource allocation between stress responses and storage-substance accumulation [45]. At early and middle grain filling, enrichment of carbon-metabolism and protein-processing pathways in Xindong 23 provides candidate processes associated with the quality contrast. Because local weather, soils and management covaried, the proposed allocation trade-off remains a hypothesis for controlled experiments.

Ribosomes serve as the core catalytic and regulatory hub for cellular protein synthesis, while the endoplasmic reticulum (ER) acts as an essential site for the synthesis, folding, and deposition of storage proteins in developing grains [46,47]. The RNA results associated ER protein processing at early filling and ribosome-related enrichment at middle filling with the Xindong 23 site response. Translation-related annotations were also present among highly connected red-module candidates. Direct transcript–protein comparison showed positive effect correlations, particularly at middle filling, while protein GO profiles emphasized stimulus-response functions. Together, these observations identify candidate relationships between protein synthesis, processing and cultivar-specific quality differences, motivating functional analysis of the corresponding genes and proteins.

Gluten proteins, particularly HMW-GS, have long been considered important determinants of wheat processing quality, whereas the effects of gliadin fractions depend on subunit composition and their balance with glutenins [48–50]. In this study, the omega-gliadin candidate *TraesCS1D02G000582*/A0A3B5ZM30 showed concordant positive transcript and protein site effects in Xindong 23 at middle filling. This association suggests that storage-protein expression patterns merit consideration alongside the observed dough properties. Their contribution to gluten-network density, cross-linking and viscoelasticity remains to be evaluated through targeted composition and polymer analyses. Thus, the present findings complement earlier work on subunit-specific gliadin effects without implying that gliadins are uniformly beneficial or detrimental.

During the late grain-filling stage (nominal 30 DAA), stage-specific molecular responses provided further context for the quality differences between the two environments. The Xindong 23 site contrast contained fewer RNA and protein discoveries than at earlier

stages, whereas Xindong 53 retained a substantial transcript response. Photosynthesis-related enrichment in Xindong 53 and stress-related annotations in Xindong 23 suggest different developmental response patterns. Collectively, differential expression and enrichment of carbohydrate metabolism, protein processing and stress-response functions identify candidate processes associated with cultivar-specific quality variation. Actual late-stage sampling was 31 DAA in Yili and 30 DAA in Tacheng, which should be considered in interpreting these profiles.

Based on the genotypic characteristics and multi-omics molecular profiles of the two cultivars, this study provides preliminary priorities for regional cultivar and field-management trials in Xinjiang. The higher values of several quality traits in Tacheng suggest that Xindong 23 merits further testing for premium bread and noodle production under comparable growing conditions. Xindong 53 offers a contrasting response profile for comparison in the same multi-environment trials. Field-management trials could evaluate nitrogen and sulphur supply, water management and disease control alongside cultivar selection; the present site comparison does not establish specific management prescriptions.

The findings concern one season and two composite site environments. Cultivar selection followed quality screening, and the three grain-filling samples were repeated collections from the same plots. Network outputs provide exploratory associations, while single-well qRT-PCR remains conditional because reference stability, amplification efficiency and amplicon specificity were not established. These limitations define priorities for independent environmental and functional validation.

5. Conclusions

By integrating multi-omics analyses of two wheat cultivars grown in two ecologically divergent regions, this study identified cultivar-specific site responses and genotype-by-site interactions for six of eight processing-quality traits. Phenotypic and multi-omics data showed larger site-associated differences in several rheological traits in Xindong 23, with stage-specific molecular associations. In Xindong 23, ER protein processing at early filling and ribosome-related pathways at middle filling were enriched, with positive transcript–protein effect agreement at these stages. A concordant omega-gliadin candidate offers a specific storage-protein association for further investigation. In contrast, Xindong 53 showed smaller site differences in several quality traits within the two-site trial.

These findings provide preliminary evidence for further environmental trials and quality-oriented breeding of wheat. From a practical perspective, they motivate further comparison of these contrasting cultivars across additional seasons and locations. Furthermore, the identified co-expression candidates and pathways require functional evaluation before application to breeding or cultivation regulation.

Supplementary Materials: The following supporting information can be downloaded at: https://www.mdpi.com/article/10.3390/agronomy16212251/s1, Table S1: quality measurements, blocked-model contrasts, diagnostics and screening sensitivity; Table S2: trial-site weather and actual sampling dates; Table S3: confirmed grain dimensions and 1000-kernel weight; Table S4: exploratory WGCNA module outputs and candidate rankings; Table S5: direct transcript–protein integration and GO intersections; Table S6: submitted primer sequences and target IDs; Table S7: candidate transcript profiles, raw Cq pairs and complementary qRT-PCR statistics. Supplementary Dataset S1: contains complete RNA/protein differential results; Dataset S2: contains complete GO/KEGG results, inputs, backgrounds and reference mappings. Figure S1: shows omics interaction effects; Figure S2: shows matched RNA–protein site effects; Figure S3: shows Xindong 53 RNA volcano plots; Figure S4: shows complementary qRT-PCR effect confidence intervals. Supplementary Methods describe statistical implementation and provenance.

Author Contributions: Conceptualization, M.Y. and X.Z.; methodology, A.Z., Y.R. and L.L.; software, A.Z. and L.L.; validation, J.C. and N.L.; formal analysis, A.Z.; investigation, A.Z., Y.R., L.L., J.C., N.L., H.Y., N.S., Y.S., Q.H. and L.W.; resources, N.S., Y.S., L.W., M.Y. and X.Z.; data curation, A.Z., Y.R., J.C., H.Y. and L.W.; writing—original draft preparation, A.Z.; writing—review and editing, H.Y., N.S., Q.H., M.Y. and X.Z.; visualization, A.Z. and Y.R.; supervision, M.Y. and X.Z.; project administration, Y.R. and N.L.; funding acquisition, M.Y. and X.Z. All authors have read and agreed to the published version of the manuscript.

Funding: This research was funded by the Fund for Stable Support to Agricultural Sci-Tech Renovation of the Xinjiang Academy of Agricultural Sciences (xjnkywdzc-2026001-4-1-5 and xjnkywdzc-2025001-18) and the Xinjiang Talent Development Fund (XJRC-2025-KJ-YJ-CXPT-049).

Data Availability Statement: The original data presented in the study are openly available in the Genome Sequence Archive (GSA), National Genomics Data Center (NGDC) at https://ngdc.cncb.ac.cn/gsa/browse/CRA050559 (accessed on 13 October 2026), under accession CRA050559 and the NGDC OMIX at https://ngdc.cncb.ac.cn/omix/release/OMIX021237 (accessed on 13 October 2026), under accession OMIX021237.

Acknowledgments: The authors gratefully acknowledge Wang Junying of the Institute of Biotechnology, Chinese Academy of Agricultural Sciences, for her help in experimental design, data analysis, and manuscript revision.

Conflicts of Interest: The authors declare no conflicts of interest.

Abbreviations

The following abbreviations are used in this manuscript:

AACC	American Association of Cereal Chemists
CDS	coding sequence
DAA	days after anthesis
DEG	differentially expressed gene
DEP	differentially expressed protein
ER	endoplasmic reticulum
FDR	false discovery rate
FPKM	fragments per kilobase of transcript per million mapped reads
G × E	genotype-by-environment
GO	Gene Ontology
HMW-GS	high-molecular-weight glutenin subunit
KEGG	Kyoto Encyclopedia of Genes and Genomes
LMW-GS	low-molecular-weight glutenin subunit
MS/MS	tandem mass spectrometry
nanoLC	nano-liquid chromatography
PCR	polymerase chain reaction
PCA	principal component analysis
qRT-PCR	quantitative real-time polymerase chain reaction
RNA-seq	RNA sequencing
WGCNA	weighted gene co-expression network analysis
BH	Benjamini–Hochberg
Cq	quantification cycle
DIA	data-independent acquisition
kME	module eigengene membership
kWithin	within-module connectivity

References

1. Shewry, P.R. Wheat in 2025: Challenges for Sustainable Production and Consumption. *J. Exp. Bot.* **2026**, *77*, 2617–2625. [CrossRef]
2. Zeibig, F.; Kilian, B.; Özkan, H.; Pantha, S.; Frei, M. Grain quality traits within the wheat (*Triticum* spp.) genepool: Prospects for improved nutrition through de novo domestication. *J. Sci. Food Agric.* **2024**, *104*, 4400–4410. [CrossRef]
3. Shen, L.; Qi, X.; Guo, Z. Wheat. *Curr. Biol.* **2025**, *35*, R1037–R1043. [CrossRef]

4. Jiang, Y.; Wang, X.D. A Brief Analysis of the Current Problems and Countermeasures of China's Wheat Industry Development. *South. Agric.* **2020**, *14*, 31–34+46.
5. Niu, L.Y.; Wang, W.W.; Zhang, Y.J.; Zou, J.W.; Wang, Z.; Lu, L.; Wang, F.Z.; Wang, W.; Yu, L. Wheat Quality and Yield Traits: Effects on Scores of Steamed Bread and Noodles. *Chin. Agric. Sci. Bull.* **2022**, *38*, 129–133.
6. Wang, Y.; Ou, X.; He, H.J.; Kamruzzaman, M. Advancements, limitations and challenges in hyperspectral imaging for comprehensive assessment of wheat quality: An up-to-date review. *Food Chem. X* **2024**, *21*, 101235. [CrossRef]
7. Tian, J.C.; Hu, R.B.; Deng, Z.Y.; Wang, Y.X. The variation and stability analysis of wheat dough stability time. *Agric. Sci. China* **2007**, *6*, 143–149. [CrossRef]
8. Kelly, J.M.; Bohman, B.; Bennett, D.; Taylor, N.L. Rapid dough making quality analysis of wheat flour using Fourier transform infrared spectroscopy and chemometrics. *Food Chem.* **2025**, *475*, 143335. [CrossRef]
9. *GB/T 17320-2013*; Quality Classification of Wheat Varieties; General Administration of Quality Supervision. Standardization Administration: Beijing, China, 2013.
10. Sun, C.; Jing, Z.; Chen, X.; Chen, J.; Shang, Q.; Jin, H.; Jia, J.; Ren, Y.; Zhao, L.; Gao, L.; et al. Reconciliation of wheat 660K and 90K SNP arrays and their utilization in dough rheological properties of bread wheat. *J. Adv. Res.* **2025**, *77*, 1–13. [CrossRef]
11. Yang, C.; Huang, L.; Wang, B.C.; Zhong, Y.; Ma, X.; Zhang, C.; Sun, Q.; Wu, Y.; Yao, Y.; Liu, Q. Enhancing quality traits in staple crops: Current advances and future perspectives. *J. Genet. Genom.* **2025**, *52*, 1438–1459. [CrossRef]
12. Shewry, P.R.; Halford, N.G.; Lafiandra, D. Genetics of wheat gluten proteins. *Adv. Genet.* **2003**, *49*, 111–184. [CrossRef]
13. Peng, Y.; Zhao, Y.; Yu, Z.; Zeng, J.; Xu, D.; Dong, J.; Ma, W. Wheat Quality Formation and Its Regulatory Mechanism. *Front. Plant Sci.* **2022**, *13*, 834654. [CrossRef]
14. Suchy, J.; Lukow, O.M.; Fu, B.X. Quantification of monomeric and polymeric wheat proteins and the relationship of protein fractions to wheat quality. *J. Sci. Food Agric.* **2003**, *83*, 1083–1090. [CrossRef]
15. Pourmohammadi, K.; Abedi, E.; Hashemi, S.M.B. Gliadin and glutenin genomes and their effects on the technological aspect of wheat-based products. *Curr. Res. Food Sci.* **2023**, *7*, 100622. [CrossRef]
16. Rasheed, A.; Xia, X.; Yan, Y.; Appels, R.; Mahmood, T.; He, Z. Wheat seed storage proteins: Advances in molecular genetics, diversity and breeding applications. *J. Cereal Sci.* **2014**, *60*, 11–24. [CrossRef]
17. Goldasteh, M.; Mehregan, I.; Naghavi, M.; Nejadsattari, T. Molecular characterization of low molecular weight glutenin (LMW) Genes in Triticeae Species with D Genome. *J. Agric. Sci. Technol.* **2019**, *21*, 1287–1299.
18. Waga, J.; Skoczowski, A. Development and characteristics of ω-gliadin-free wheat genotypes. *Euphytica* **2014**, *195*, 105–116. [CrossRef]
19. Van den Broeck, H.C.; Gilissen, L.J.; Smulders, M.J.; van der Meer, I.M.; Hamer, R.J. Dough quality of bread wheat lacking α-gliadins with celiac disease epitopes and addition of celiac-safe avenins to improve dough quality. *J. Cereal Sci.* **2011**, *53*, 206–216. [CrossRef]
20. Zhou, Z.; Liu, C.; Qin, M.; Li, W.; Hou, J.; Shi, X.; Dai, Z.; Yao, W.; Tian, B.; Lei, Z.; et al. Promoter DNA hypermethylation of *TaGli-γ-2.1* positively regulates gluten strength in bread wheat. *J. Adv. Res.* **2021**, *36*, 163–173. [CrossRef]
21. Guo, W.; Yang, H.; Liu, Y.; Gao, Y.; Ni, Z.; Peng, H.; Xin, M.; Hu, Z.; Sun, Q.; Yao, Y. The wheat transcription factor *TaGAMyb* recruits histone acetyltransferase and activates the expression of a high-molecular-weight glutenin subunit gene. *Plant J.* **2015**, *84*, 347–359. [CrossRef]
22. Gao, Y.; An, K.; Guo, W.; Chen, Y.; Zhang, R.; Zhang, X.; Chang, S.; Rossi, V.; Jin, F.; Cao, X.; et al. The endosperm-specific transcription factor *TaNAC019* regulates glutenin and starch accumulation and its elite allele improves wheat grain quality. *Plant Cell* **2021**, *33*, 603–622. [CrossRef]
23. Nuttall, J.C.; Oleary, G.J.; Panozzo, J.F.; Walker, C.K.; Barlow, K.M.; Fitzgerald, G.J. Models of grain quality in wheat-a review. *Field Crops Res.* **2017**, *202*, 136–145. [CrossRef]
24. Zahra, N.; Hafeez, M.B.; Wahid, A.; Al Masruri, M.H.; Ullah, A.; Siddique, K.H.M.; Farooq, M. Impact of climate change on wheat grain composition and quality. *J. Sci. Food Agric.* **2023**, *103*, 2745–2751. [CrossRef]
25. Yang, H.; Li, Y.; Zhao, J.; Chen, Z.; Huang, X.; Fan, G. Regulating the composition and secondary structure of wheat protein through canopy shading to improve dough performance and nutritional index. *Food Res. Int.* **2023**, *173*, 113399. [CrossRef]
26. Gu, A.; Hao, P.; Lv, D.; Zhen, S.; Bian, Y.; Ma, C.; Xu, Y.; Zhang, W.; Yan, Y. Integrated Proteome Analysis of the Wheat Embryo and Endosperm Reveals Central Metabolic Changes Involved in the Water Deficit Response during Grain Development. *J. Agric. Food Chem.* **2015**, *63*, 8478–8487. [CrossRef]
27. Ghafoor, A.Z.; Ceglińska, A.; Karim, H.; Wijata, M.; Sobczyński, G.; Derejko, A.; Studnicki, M.; Rozbicki, J.; Cacak-Pietrzak, G. Influence of Genotype, Environment, and Crop Management on the Yield and Bread-Making Quality in Spring Wheat Cultivars. *Agriculture* **2024**, *14*, 2131. [CrossRef]
28. *AACC Method 39-11*; Near-Infrared Reflectance Method for Protein Determination in Wheat Flour. American Association of Cereal Chemists: St. Paul, MN, USA, 1999.
29. *AACC Method 38-12*; Wet Gluten and Gluten Index. American Association of Cereal Chemists: St. Paul, MN, USA, 1999.

30. *GB/T 14614-2019*; Inspection of Grain and Oils-Doughs Rheological Properties Determination of Wheat Flour-Farinograph Test. State Administration for Market Regulation. Standardization Administration: Beijing, China, 2019.
31. *GB/T 14615-2019*; Inspection of Grain and Oils-Doughs Rheological Properties Determination of Wheat Flour-Extensograph Test. State Administration for Market Regulation. Standardization Administration: Beijing, China, 2019.
32. Chen, S.; Zhou, Y.; Chen, Y.; Gu, J. fastp: An Ultra-Fast All-in-One FASTQ Preprocessor. *Bioinformatics* **2018**, *34*, i884–i890. [CrossRef]
33. Kim, D.; Paggi, J.M.; Park, C.; Bennett, C.; Salzberg, S.L. Graph-based genome alignment and genotyping with HISAT2 and HISAT-genotype. *Nat. Biotechnol.* **2019**, *37*, 907–915. [CrossRef]
34. Pertea, M.; Pertea, G.M.; Antonescu, C.M.; Chang, T.-C.; Mendell, J.T.; Salzberg, S.L. StringTie Enables Improved Reconstruction of a Transcriptome from RNA-Seq Reads. *Nat. Biotechnol.* **2015**, *33*, 290–295. [CrossRef]
35. Love, M.I.; Huber, W.; Anders, S. Moderated estimation of fold change and dispersion for RNA-seq data with DESeq2. *Genome Biol.* **2014**, *15*, 550. [CrossRef]
36. Zhao, Y.; Li, M.C.; Konaté, M.M.; Chen, L.; Das, B.; Karlovich, C.; Williams, P.M.; Evrard, Y.A.; Doroshow, J.H.; McShane, L.M. TPM, FPKM, or Normalized Counts? A Comparative Study of Quantification Measures for the Analysis of RNA-seq Data from the NCI Patient-Derived Models Repository. *J. Transl. Med.* **2021**, *19*, 269. [CrossRef]
37. Sun, N.; Liu, W.; Xu, W.; Li, L.; Yuan, T.; Chen, L. Comparative Proteomic Analysis Reveals That *TaCAD-A1* Enhances Resistance of Wheat to Powdery Mildew (*Blumeria graminis* f. sp. *tritici*). *Life* **2026**, *16*, 872. [CrossRef]
38. Livak, K.J.; Schmittgen, T.D. Analysis of relative gene expression data using real-time quantitative PCR and the 2(-Delta Delta C(T)) Method. *Methods* **2001**, *25*, 402–408.
39. Götz, S.; Arnold, R.; Sebastián-León, P.; Martín-Rodríguez, S.; Tischler, P.; Jehl, M.A.; Dopazo, J.; Rattei, T.; Conesa, A. B2G-FAR, a species-centered GO annotation repository. *Bioinformatics* **2011**, *27*, 919–924. [CrossRef]
40. Kanehisa, M.; Sato, Y. KEGG Mapper for inferring cellular functions from protein sequences. *Protein Sci.* **2020**, *29*, 28–35. [CrossRef]
41. Rhazi, L.; Méléard, B.; Daaloul, O.; Grignon, G.; Branlard, G.; Aussenac, T. Genetic and Environmental Variation in Starch Content, Starch Granule Distribution and Starch Polymer Molecular Characteristics of French Bread Wheat. *Foods* **2021**, *10*, 205. [CrossRef]
42. Hellemans, T.; Landschoot, S.; Dewitte, K.; Van Bockstaele, F.; Vermeir, P.; Eeckhout, M.; Haesaert, G. Impact of Crop Husbandry Practices and Environmental Conditions on Wheat Composition and Quality: A Review. *J. Agric. Food Chem.* **2018**, *66*, 2491–2509. [CrossRef]
43. Hnizil, O.; Baidani, A.; Khlila, I.; Taghouti, M.; Nsarellah, N.; Amamou, A. Dissecting Genotype by Environment Interactions in Moroccan Wheat: An Advanced Biplot and Heatmap Analysis Unveiling Agronomic, Quality Traits, and Genotypic Stability for Tailored Breeding Strategies. *Plants* **2024**, *13*, 1068. [CrossRef]
44. Filip, E.; Woronko, K.; Stępień, E.; Czarniecka, N. An Overview of Factors Affecting the Functional Quality of Common Wheat (*Triticum aestivum* L.). *Int. J. Mol. Sci.* **2023**, *24*, 7524. [CrossRef]
45. Simón, M.R.; Fleitas, M.C.; Castro, A.C.; Schierenbeck, M. How Foliar Fungal Diseases Affect Nitrogen Dynamics, Milling, and End-Use Quality of Wheat. *Front. Plant Sci.* **2020**, *11*, 569401. [CrossRef]
46. Doudna, J.A.; Rath, V.L. Structure and function of the eukaryotic ribosome: The next frontier. *Cell* **2002**, *109*, 153–156.
47. Schwarz, D.S.; Blower, M.D. The endoplasmic reticulum: Structure, function and response to cellular signaling. *Cell Mol. Life Sci.* **2016**, *73*, 79–94. [CrossRef]
48. Buttar, Z.A.; Shalmani, A.; Niaz, M.; Wang, C.; Hussain, S.; Wang, C. Transcriptome Analysis Reveals Potential Mechanism in Storage Protein Trafficking within Developing Grains of Common Wheat. *Int. J. Mol. Sci.* **2022**, *23*, 14851. [CrossRef]
49. Lv, L.; Zhao, A.; Zhang, Y.; Li, H.; Chen, X. Proteome and transcriptome analyses of wheat near isogenic lines identifies key proteins and genes of wheat bread quality. *Sci. Rep.* **2021**, *11*, 9978. [CrossRef]
50. Khalid, A.; Hameed, A.; Tahir, M.F. Wheat quality: A review on chemical composition, nutritional attributes, grain anatomy, types, classification, and function of seed storage proteins in bread making quality. *Front. Nutr.* **2023**, *10*, 1053196. [CrossRef]

Disclaimer/Publisher's Note: The statements, opinions and data contained in all publications are solely those of the individual author(s) and contributor(s) and not of MDPI and/or the editor(s). MDPI and/or the editor(s) disclaim responsibility for any injury to people or property resulting from any ideas, methods, instructions or products referred to in the content.